Time-Resolved Titrations of ASP-85 in Bacteriorhodopsin: The Multicomponent Kinetic Mechanism†

N. Friedman,‡ I. Rousso,‡ M. Sheves,*,‡ X. Fu,§ S. Bressler,§ S. Druckmann,§ and M. Ottolenghi*,§

Department of Organic Chemistry, The Weizmann Institute of Science, Rehovot 76100, Israel, and Department of Physical Chemistry, The Hebrew University, Jerusalem 91904, Israel

Received March 20, 1997; Revised Manuscript Received June 30, 1997⊗

ABSTRACT: The Asp-85 residue, located in the vicinity of the retinal chromophore, plays a key role in the function of bacteriorhodopsin (bR) as a light-driven proton pump. In the unphotolyzed pigment the protonation of Asp-85 is responsible for the transition from the purple form (λ_{max} = 570 nm) to the blue form (λ_{max} = 605 nm) of bR (pK_a = 3.5 in 20 mM NaCl). The Purple⇔Blue transition can also be induced by deionization (cation removal). These color changes offer a unique opportunity for time resolving the titration of a protein residue using conventional stopped-flow methodologies. We have studied the Purple⇔Blue equilibration kinetics in bR by exposing the system to pH and to cation jumps. Independently of the equilibration direction (Purple→Blue or Blue→Purple) and of the inducing concentration jump ([H^+] or [cation]), the kinetics are found to exhibit analogous multicomponent features. Analysis of the data over a range of cation concentrations and pH values leads to the conclusion that the rate-determining step in the overall titration of Asp-85 is proton translocation through a specific proton channel. The multicomponent kinetics, extending over a wide time range (10^{-2}−10^4 s), are accounted for in terms of a pH-dependent heterogeneity of proton channels. A model is presented in which the relative weight of four proton channels is determined by the state of protonation of two interacting, channel-controlling, protein residues A_1 and A_2. These findings bear on the mechanism of the vectorial proton translocation associated with the photocycle of bR.

The molecular mechanism of the light-induced proton pump, bacteriorhodopsin (bR), is controlled by a series of proton translocation reactions involving several amino acids, as well as the Schiff base (SB) which links the retinal chromophore to the Lys-216 protein residue. [For a recent series of review articles on bR and other retinal proteins see Ottolenghi, M. and Sheves, M., Eds. (1995) Photophysics and Photochemistry of Retinal Proteins. *Isr. J. Chem. 35* (3−4), 193−515.] Mechanistic key roles are played by the (protonated) Schiff base and by its neighboring Asp-85 residue which is located closer to the extracellular side of the membrane (Henderson et al., 1990). During the M stage of the photocycle, at neutral pH, a proton is translocated from the SB to Asp-85 inducing a proton release from a group suggested to be Glu-204 (Brown et al., 1995) to the extracellular medium, thus initiating the proton pump mechanism which is completed by uptake from the cytoplasmic side. At low pH, below the pK_a of the proton releasing group in M, proton uptake from the cytoplasmic side precedes the release reaction (Zimanyi et al., 1992), suggesting that the latter occurs directly from Asp-85. An additional critical role of Asp-85 is its postulated participation in the "reprotonation switch" which during the photocycle changes the proton accessibility of the SB from the extracellular side to the cytoplasmic side. [For a recent review see Honig et al. (1995).]

The direct role of Asp-85 in the light-induced function of bR has stimulated extensive work related to its role in determining the structure and spectrum of the nonphotolyzed pigment. Primarily, the transition from the purple (high pH) form of bR to its blue (low pH) form (Oesterhelt & Stoeckenius, 1971; Moore et al., 1978) was found to be associated with protonation of the negative Asp-85 residue, in the vicinity of the chromophore (Mowery et al., 1979; Fisher & Oesterhelt, 1979; Warshel & Ottolenghi, 1979; Nakanishi et al., 1980; Subramaniam et al., 1990; Metz et al., 1992; Masuda et al., 1995). An analogous Purple→Blue transition can also be induced by deionization (cation removal) rather than by acidification (Kimura et al., 1984; Chang et al., 1985; El Sayed et al., 1995). The binding of metal cations to bR, and the way they control the state of protonation of Asp-85, was first interpreted in terms of the effects of free or bound cations on the membrane surface (Kimura et al., 1984; Chang et al., 1986; Ariki et al., 1987; Dunach et al., 1987; Concoran et al., 1987; Szundi & Stoeckenius, 1987, 1988, 1989). It was later claimed that apart from the surface charge (which lowers the surface pH causing protonation of Asp-85) cation binding at specific negative protein sites should also play a critical role (Ariki & Lanyi, 1986). It was later suggested (Jonas & Ebrey, 1991; Zhang et al., 1992; Stuart et al., 1995; El-Sayed et al., 1995; Birge et al., 1996) that the purple color of bR is determined by a divalent cation interacting with two negative protein residues (denoted here as Y and Z), identified respectively as Asp-85 and Asp-212 which are both located in the vicinity of the Schiff base (Grigorieff et al., 1996). Accordingly, the Purple→Blue transition is suggested

† This work was supported by the Fund for Basic Research (administered by The Israel Academy of Sciences and Humanities)—Centers of Excellence Program, by the U.S.−Israel Binational Science Foundation, and by The Farkas Center for Light Induced Processes (Minerva GmbH).

* Corresponding authors.
‡ The Weizmann Institute of Science.
§ The Hebrew University.

⊗ Abstract published in *Advance ACS Abstracts,* September 1, 1997.

[1] Abbreviations: bR, bacteriorhodopsin; SB, Schiff base; TCA, trichloroacetic acid; DA, dark-adapted; LA, light-adapted.

S0006-2960(97)00646-6 CCC: $14.00

to be associated with the uptake of two protons by these two residues and with the simultaneous unbinding of the metal cation.

Important information which is not available from equilibrium pK_a measurements may be obtained by studying the acid−base equilibration kinetics of protein residues (Honig et al., 1995). Such experiments may shed light on the accessibility of such residues to the external medium, also helping to resolve hidden (overlapping) titrations. Time-resolved titrations are usually difficult to perform in proteins. However, due to the associated changes in color, they have been carried out in bR, using conventional stopped-flow techniques, for both Schiff base (Druckmann et al., 1982, 1995; Kataoka et al., 1994) and Asp-85 (Druckmann et al., 1979, 1985, 1995; Kimura et al., 1984; Zubov et al., 1986; Kataoka et al., 1994). In the case of Asp-85 the time-resolved titrations have shown that (i) Asp-85 is exposed (to protons) to the extracellular side of the membrane; (ii) in variance with the highly exposed nature of the proton releasing group residue, the rate-determining step in the titration of Asp-85 is proton translocation along a saturable channel to the outside; (iii) and Asp-85 is an essential part of a channel which allows proton exchange between the SB and the extracellular medium (Druckmann et al., 1995).

An unexplained phenomenon which interferes with the interpretation of the time-resolved titrations of Asp-85 is the multiphasic kinetic nature of the pH-induced Purple→Blue reaction, exhibiting both slow (Moore et al., 1978) and fast (Druckmann et al., 1979, 1985) phases. Interestingly, multicomponent kinetic patterns are also observed when the Blue→Purple equilibration is induced by cation jumps (Kimura et al., 1984; Zubov et al., 1986). The question arises as to the relation that such patterns carry to those observed in the pH-induced titrations. Primarily, it is important to understand the molecular mechanism underlying the multicomponent kinetics: Is the rate of the reaction controlled by the rate of metal binding and unbinding, or by the Asp-85 protonation/deprotonation process? Are the complex features associated with different titration channels or, e.g., with cooperativity between chromophores (Druckmann et al., 1985)? We have addressed these questions by performing time-resolved titrations of Asp-85 over a wide range of pH and cation concentrations. The Purple⇔Blue transition was induced in both directions, by both pH and cation jumps. An important observation is that the kinetics of the cation-induced Blue→Purple transition is independent of the cation type and concentration. Analysis of the data leads to the following major conclusions: (i) The binding/unbinding of metal cations is not rate determining in the titration of Asp-85. The titration rate is determined by the rate of proton transfer through an appropriate proton channel. (ii) The multiexponential features of the titration are rationalized in terms of two fast proton channels, $k(F_1) = 30-80\ s^{-1}$ and $k(F_2) = 1-3\ s^{-1}$, and two slow channels, $k(S_1) \approx 10^{-2}\ s^{-1}$ and $k(S_2) \approx 10^{-3}\ s^{-1}$. The relative amounts of the two fast channels, $A(F_1 + F_2)$, and the slow channels, $A(S_1)$ and $A(S_2)$, are controlled by the state of protonation of two interacting protein residues A_1 and A_2.

MATERIALS AND METHODS

pH or cation jump experiments were carried out using a Hewlett Packard diode-array spectrophotometer or a microvolume stopped-flow reaction analyzer (Applied Photophysics Ltd., U.K., SX-17MV). All experiments were carried out by mixing equal volumes of bR suspensions with the appropriate acid, buffer, or salt solution. The spectrophotometer was used for following the slow components of the reaction above 3 s. The titration fraction occurring faster than 3 s was termed "fast" (F) while the slower components were termed "slow" (S). bR concentrations were 1.5×10^{-5} M. All salts were Fluka analytical grade.

pH jumps to low pH are associated with aggregation phenomena which increase the scattering of the solutions. Aggregation, which occurs on the time range of the S components of the titration, was taken into account by referring to wavelengths which are out of the spectral range of the Purple⇔Blue transition, namely, $\lambda < 420$ nm and $\lambda > 740$ nm. A complete spectrum, between 400 and 800 nm, was recorded for each time point. After subtraction of the $t = 0$ spectrum, a linear base line correction of the difference spectra was applied.

Deionized blue membranes were obtained by passing bR suspensions through a cation-exchange resin column (Fluka Dowex 50W×8). Such membrane suspensions (pH = 4.0−4.2) were exposed to ion jumps inducing the transition to the purple form. We were also interested in carrying out pH titrations of such deionized suspensions which are characterized by a relatively high pK_a, as compared to the parent nondeionized suspensions. With the purpose of carrying out Purple→Blue pH titrations of such deionized preparations, we have devised the following procedure for preparing deionized purple membrane suspensions (dI-bR) at a relatively high pH. After the membrane suspension was passed through the cation-exchange resin column, the resulting blue bR was treated with a 0.1 N KOH solution, adjusting the pH to ∼6 (denoted as K-bR). To this membrane suspension was added a crown ether (18-crown-6, Fluka) solution, adjusted to pH = 6, in order to complex most of the K^+ ions in the solution. The resulting (purple) membrane suspension ([bR] = 8×10^{-6} M, pH = 6, 0.2 M crown ether) was exposed to acidification experiments by adding HCl. Cation-removing jumps were performed using the above K-bR solution (1.6×10^{-5} bR, pH 6), adding to it a 0.4 M 18-crown-6 solution to final concentrations of [bR] = 0.8×10^{-5} M, [18-crown-6] = 0.2 M, and [KOH] = 6×10^{-4} M.

pK_a values of the Purple⇔Blue titration [denoted in Table 2 as pK_a(A)] were calculated by fitting the absorbance change (A) at 630 nm as a function of pH using the expression $A(\text{pH}) = A_{max}/(1 + 10^{n(pKa-pH)})$. The p$K_a$ values corresponding to the thermodynamic cycle of Scheme 1 were calculated by deriving a set of three equations representing the relative amounts of the three H^+ channel components, associated with the two protein moieties, A_1 and A_2 (see text): $\{A_1^-, A_2^-\}$ and $\{A_1H, A_2H\}$ (F channels), $\{A_1H, A_2^-\}$ (S_1 channel), $\{A_1^-, A_2H\}$ (S_2 channel). The pK_a values in the above equations were simultaneously optimized using a line search algorithm to best fit the experimental data.

RESULTS

(I) pH Jumps

Purple to Blue Transitions. (a) Multicomponent Nature of the Transitions. Purple to blue transitions in bR were induced by pH jumps in dark-adapted bR suspensions from an initial neutral ($pH_i = 7$) to a final low ($pH_f \leq 4$) pH value.

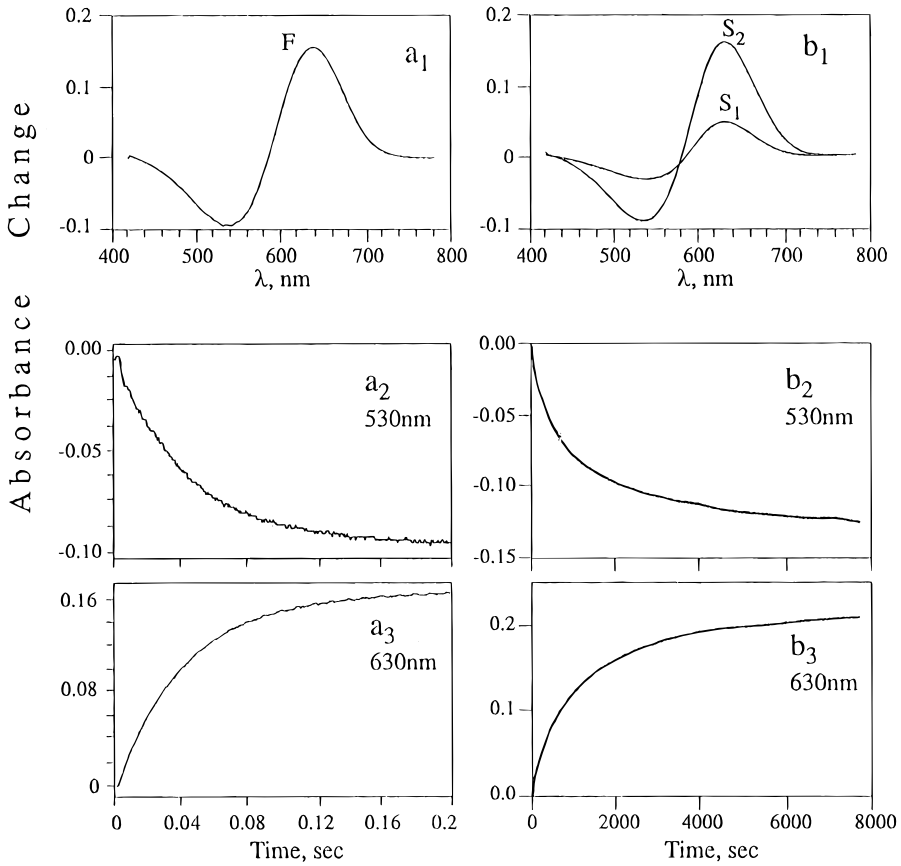

FIGURE 1: Characteristic difference spectra (a_1 and b_1) and decay traces (a_2, a_3, b_2, and b_3) showing the purple to blue transition in bR, induced by pH jumps from pH = 7 to pH = 2.4 ([bR] = 1.6×10^{-5}, 0.02 mM phthalate buffer, sodium salt. (a_1-a_3): Fast components (<3 s). (b_1-b_3) Slow components (>3 s). Corrections for scattering due to aggregation have been carried out as described in the text.

Characteristic difference spectra corresponding to the fast (<3 s) and to the slow (>3 s) components of the pH 7→pH 2.4 transitions are shown in Figures $1a_1$ and b_1. Figures $1a_2$, a_3,b_2, and b_3 show kinetic traces at the two wavelengths, 530 and 630 nm, corresponding to the maximal amplitudes in the difference spectra. It is clearly evident that the kinetics, spanning a broad time range, are multicomponent. As shown in Figure 2 very good fits were obtained using a four-exponent analysis. The quality of fits with one, two, and even three exponents was considerably lower. Adding additional components did not improve the quality of the fits (the additional amplitudes were exceedingly small). Thus, four appears to be the minimum number of exponents required to describe the reaction. As a result we have adopted the four-component approximation as a plausible working hypothesis (see Discussion below). The four rate parameters and the corresponding relative amplitudes are given in Table 1. For reasons which will be clarified below, it is convenient to denote the four components as two fast components (F_1, F_2) and two slow components (S_1, S_2). It is important to note that jumps to low pH are associated with considerable changes in scattering due to membrane aggregation phenomena. These effects have been taken into account in the analysis of our data (see Materials and Methods) so that the parameters presented in Table 1 reflect net absorbance changes, free from scattering artifacts.

(b) pH Effects. The kinetics of the Purple→Blue pH jumps were investigated over a range of final pH values (pH_f), starting from the same initial pH value ($pH_i = 7$). Figure 3 shows the pH_f dependence of the total amplitude of the titration (A), along with those of the subcomponents, A(F) = $A(F_1 + F_2)$, $A(S_1)$, and $A(S_2)$, for four characteristic acids (HCl, H_2SO_4, TCA, and phthalic acid). It is evident that marked pH effects are observed on the relative amounts of S_1, S_2, and $F = F_1 + F_2$. No substantial pH effects were found on the kinetics or on the relative amplitudes [$A(F_1)$/A(F), $A(F_2)$/A(F)] of the two fast components within the 2.4−4.5 pH range (see also Table 1). The same general features of the pH effect, namely, a monotonous increase in A(F) with decreasing pH, and peaking curves in the cases of $A(S_1)$ and $A(S_2)$ are observed for all four acids employed. However, the details of the effect depend on the specific anion. Thus, the titration-like curves of A(F) move to lower pH values in the sequence H_2SO_4, HCl, TCA, and phthalic acid. When analyzed according to the expression $A(pH) = A_{max}(1 + 10^{n(pKa-pH)})$, p$K_a$ and n values as given in Table 2 were obtained. The $n \approx 2$ value is in keeping with previous observations (Jonas & Ebrey, 1991), indicating that the Purple to Blue transition is associated with a titration involving two protons. The pK_a values (20 mM salt) in the cases of phthalate (2.7) and TCA (3.25) are substantially lower than those of chloride (3.5) and sulfate (3.5).

Figure 3 shows that the relative amounts of the F, S_1, and S_2 components do not simply follow the curve of the overall titration. It is evident that, in all cases upon lowering the pH, the evolution of the S_1 and S_2 components lags behind the F components, subsequently decreasing at lower pH values. The effect of pH on the relative amounts of the three components is best visualized by plotting the fractions of F, S_1, and S_2 against pH. As shown in Figure 4 the corresponding fractions, $A_i = A(i)/\sum A(i)$, i.e., $A_F = A(F)/[A(F) + A(S_1) + A(S_2)]$, $A_{S1} = A(S_1)/[A(F) + A(S_1) + A(S_2)]$, and $A_{S2} = A(S_2)/[A(F) + A(S_1) + A(S_2)]$, exhibit complementary "bell-shaped" curves. It is thus evident that the increase in

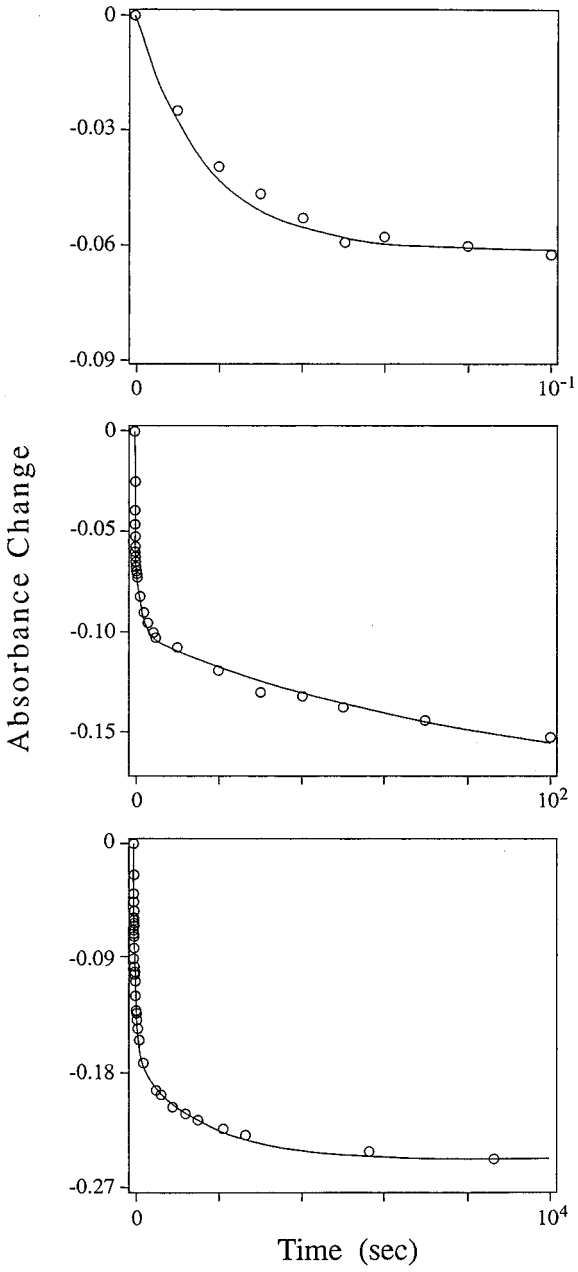

FIGURE 2: Experimental points and curves (solid lines) calculated on the basis of a four-exponential fit in the case of a characteristic Blue→Purple (10:1, Ca^{2+}:bR) cation jump. Figure shows three representative time scales.

A_{S1} and A_{S2} in the low pH range and their decrease at high pH are associated with a complementary decrease and increase in A_F, respectively. As mentioned above $A(F_1)$ and $A(F_2)$ exhibit an analogous pH dependence, namely, their relative contribution is pH_f independent.

A pH dependence was also found for the rate constants of the two slow decay components $k(S_1)$ and $k(S_2)$. As shown in Figure 5 both rate constants increase in the range below pH ≈ 3.2, which qualitatively corresponds to the low pH range of the bell-shaped curves of Figure 4. In contrast to this behavior essentially no pH_f effects were observed on $k(F_1)$ and $k(F_2)$ in the above pH range. Moreover, in variance with the effects of the specific anion on the overall pK_a of the titration and on the relative contributions of S_1, S_2, and F, no anion effects were observed on the values of $k(F_1)$ and $k(F_2)$. Thus, the following values were obtained for a jump from $pH_i = 7$ to $pH_f = 2.45$: $k(F_1) = 30.0 \pm 3.0$, 32.0 ± 3.0, 36.0 ± 3.0, 33.0 ± 3.0, and $k(F_2) = 4.0 \pm 2.0$,

Table 1: Representative Data Showing the Results of a Four-Component Kinetic Analysis of the Purple→Blue and Blue→Purple Transitions in bR[g]

	Purple→Blue									Blue→Purple								
	pH jumps						cation jumps[e]			pH jumps				Ca^{2+} jumps[d]				
	7→2.4[a]		7→3.3		6.0→3.5[c]					2.6→3.6		2.6→6.2		DA		LA		
component	k	A	k	A	k	A	k	A		k	A	k	A	k	A	k	A	
F_1	26	0.35	32[a]	0.55[f]	42	0.8	–	0.8 (F_1 + F_2)		70	0.22	80	0.42	64	0.24	62	0.25	
			45[a,b]															
F_2	3.5	0.06	1.0[a]	0.1[f]	3.1	0.15	–			0.4	0.19	0.8	0.38	0.8	0.17	0.9	0.16	
S_1	7×10^{-3}	0.14	1.6×10^{-2}[f]	0.1[f]	2.2×10^{-2}	0.05	2.5×10^{-2}	0.2		8.5×10^{-3}	0.28	~10^{-2}	0.1	1.3×10^{-2}	0.29	1.2×10^{-2}	0.30	
S_2	5.8×10^{-4}	0.45	1.7×10^{-3}[f]	0.25[f]	–	<0.01	–	–		4×10^{-4}	0.3	–	<0.01	5.6×10^{-4}	0.30	4.6×10^{-4}	0.29	

[a] Phthalate buffer. [b] $pH_f = 3.9$. [c] Deionized purple bR (dI-PbR). [d] Ca^{2+} jumps correspond to a 10:1 [Ca^{2+}]:[bR] ratio. DA and LA denote dark and light-adapted blue membrane suspensions, respectively. $pH_i = 4.0-4.2$, $pH_f = 3.7-3.8$. [e] Induced by rapid mixing of the purple suspension with a 18-crown-6 ether solution. [f] HCl. [g] Transitions are induced either by pH or by cations jumps. k Values are the rate constants in s^{-1}. A denotes the corresponding amplitude fractions at 630 nm. Error estimates are on the order of 10% (amplitudes) or 30% (rate constants).

Table 2: pK_a Values of Protein Residues (Y and Z) Responsible for the Overall Purple⇔Blue Transition (p$K_a(A)$) and of Residues Controlling the Kinetic Components of the Titration (A_1 and A_2)[a]

titration parameter	titrated groups	HCl	H_2SO_4	TCA	phthalate	HCl (deionized)
pK_a (*A*)	Y, Z	3.50 ± 0.04 $n = 1.9 \pm 0.3$	3.54 ± 0.04 $n = 2.0 \pm 0.3$	3.15 ± 0.05 $n = 2.0 \pm 0.3$	2.70 ± 0.07 $n = 1.7 \pm 0.3$	4.6 ± 0.2 $n = 1.5 \pm 0.3$
pK_a (1)	A_1 (with A_2H)	3.07	3.05	2.57	2.26	5.74
pK_a (2)	A_1 (with A_2^-)	3.22	3.08	2.18	2.44	4.33
pK_a (3)	A_2 (with A_1H)	3.20	3.26	3.42	2.66	5.03
pK_a (4)	A_2 (with A_1^-)	3.35	3.30	3.03	2.84	3.62

[a] The four pK_a values, pK_a(1) to pK_a(4), are calculated according to the model of Scheme 1 to fit the experimental values of A_F, A_{S1}, and A_{S2} shown in Figure 4. The model assumes that the relative contributions of A_F, A_{S1}, A_{S2}, are proportional to the relative amount of states I and states IV, II, and III (see text), respectively. The pK_a(1)−pK_a(4) values are subject to the restriction pK_a(1) + pK_a(4) = pK_a(2) + pK_a(3).

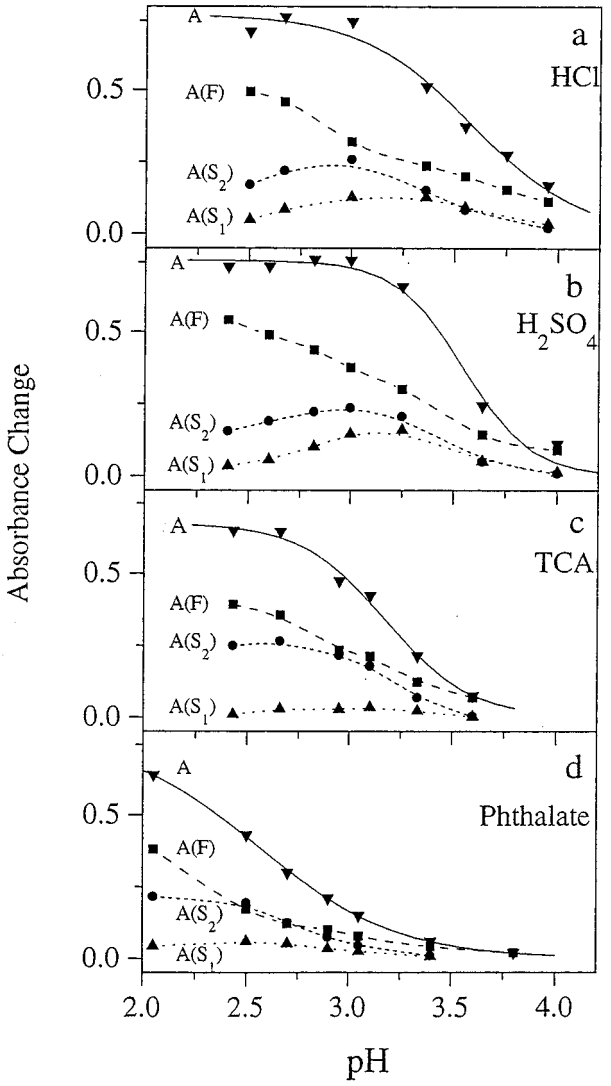

FIGURE 3: pH and anion dependence of the total amplitude (A) and subcomponents [$A(F) = A(F_1 + F_2)$, $A(S_1)$, and $A(S_2)$] of the pH-induced Purple→Blue transition in bR. The *A* parameters correspond to the absorbance changes of the transition monitored at 630 nm. The solid lines in the case of the *A* curves correspond to the titration curve fits (see text). Titrations from $pH_i = 7$ were carried out with (a) HCl (+ 0.02 M NaCl); (b) H_2SO_4 (+ 0.01 M Na_2SO_4); (c) TCA (+ 0.02 M NaTCA); (d) 0.02 M phthalate buffer (sodium salt).

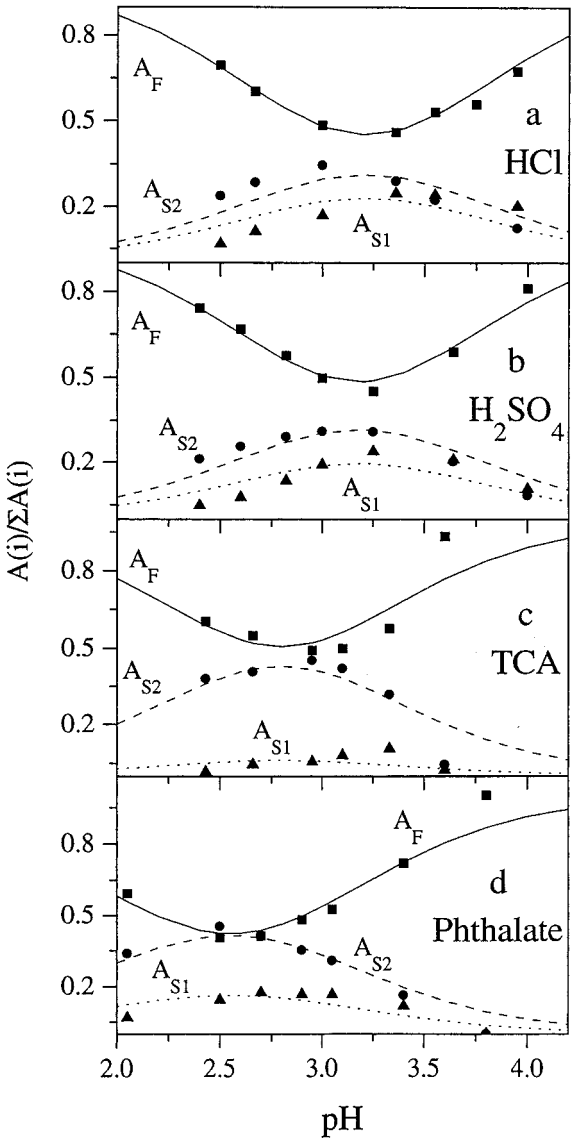

FIGURE 4: pH_f and anion dependence of the relative amounts (fractions) of the various components of the Purple to Blue transition. Fractions (A_F, A_{S1}, A_{S2}) are defined as $A_i = A(i)/\Sigma A(i)$. Data are the same as in Figure 2. (□) A_F; (○) and A_{S2}; (△) A_{S1}. The lines are calculated according to the model of Scheme 1 to fit the experimental points. The pK_a values obtained in these fits are given in Table 2.

3.6 ± 2.0, 5.3 ± 2.0, 3.8 ± 2.0, using HCl, H_2SO_4, H_3PO_4, and TCA, respectively. In all cases the value of $A(F_1)/A(F_1 + F_2)$ was 0.8 ± 0.08. These parameters are essentially identical to those reported for phthalic acid in Figure 5 and in Table 1.

We finally note that when acidification experiments are carried out at pH values which are at the onset of the Purple→Blue transition (pH 4−5) an additional transition is observed associated with an absorption increase at 480 nm and a decrease at 580 nm. This transition occurs on a time range comparable to that of the S components. However, it is small in amplitude (~5% relative to that of the Purple⇔Blue titration) and therefore did not interfere with our analysis of the Asp-85 titration.

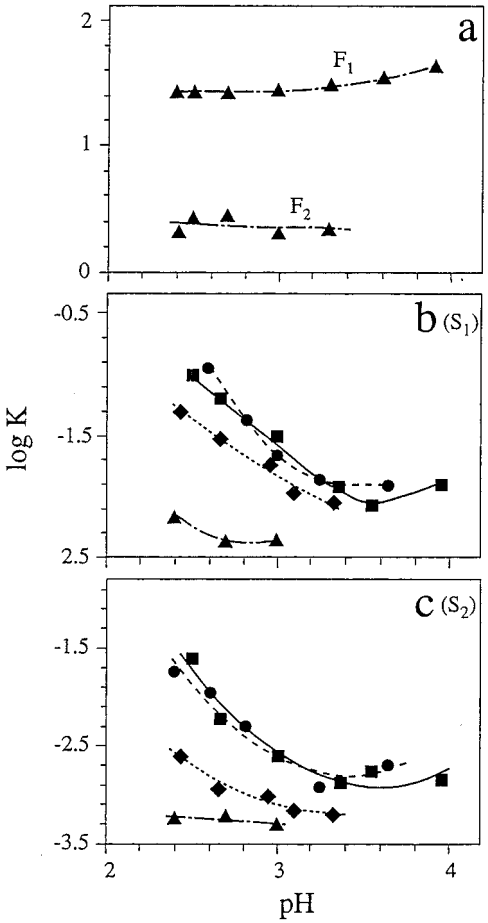

FIGURE 5: Effect of pH_f and of the specific anion on the rates of the slow components, S_1 (b) and S_2 (c), in the pH-induced Purple→Blue transition. (□) HCl; (○) H_2SO_4; (◆) TCA, (△) phthalate buffer. Data for the fast components, F_1 and F_2 (phthalate buffer), are also included (a).

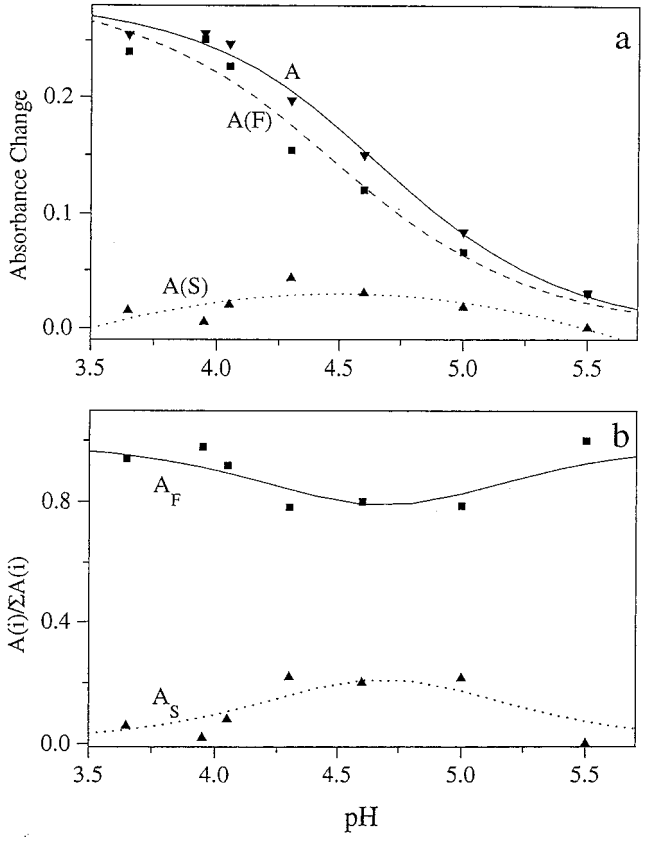

FIGURE 6: Titration of purple deionized bR. The Purple→Blue transition is induced by acidification with HCl. Absorbance changes monitored at 630 nm. (a) (▽) Overall titration (A), (□) fast Components ($A(F) = A(F_1 + F_2)$); and (△) slow Components ($A(S)$). (b) Relative amount of the fast components, $A_F = (A(F)/(A(F) + A(S))$, and of the slow components, $A_S = A(S)/A(F) + A(S)$. The lines have been calculated using the model of Scheme 1 (see legend to Figure 3).

(c) Effects of Dark→Light Adaptation. The isomer composition of dark-adapted bR at neutral pH is 40% *all-trans* and 60% 13-*cis* (Scherrer & Stoeckenius, 1985). The question arises as to whether the multiphasic nature of the Purple to Blue transition may be associated with such isomer heterogeneity of the dark-adapted membrane. We addressed the problem by carrying out pH jumps, analogous to those described above, with samples light-adapted at $pH_i = 7$, which are exclusively *all-trans*. A characteristic jump to pH = 2.4 (phthalate buffer) yields rate parameters $k(F_1) = 32.0 \pm 4.0\ s^{-1}$, $k(F_2) = 6.0 \pm 3.0\ s^{-1}$ [$A(F_1)/A(F_1 + F_2) = 0.8 \pm 0.08$], which are analogous to those of the dark-adapted samples (see Table 1). We conclude that the nature of the specific isomer, 13-*cis* or *all-trans*, has no effect on the kinetics of the fast components of the Purple→Blue transition. As to the slow components, these were also present in the light-adapted system but could not be quantitatively analyzed due to the interfering effects of the light to dark adaptation kinetics. Thus, a*ll-trans*→13-*cis* isomerization at neutral pH occurs on a time scale (∼1 h) which is longer than that of the F and S_1 components of the Purple→Blue titration (but which overlaps with S_2). Isomerization is accelerated at low pH due to the catalytic effect of protonation of Asp-85, i.e., of the generation of the blue form (Balashov et al., 1993). In this case it overlaps with the S_1 kinetics.

(d) Titration of Deionized Purple Membranes. It is well established that upon cation removal the apparent pK_a of the Purple⇔Blue transition in bR shifts from around 3, in the presence of 100 mM salt, to higher values (Kimura et al., 1984; Jonas & Ebrey, 1991). Analogously to the experiments described above for nondeionized bR, we have carried out Purple→Blue titrations of deionized high-pK_a preparations using the crown ether method described in Materials and Methods. As shown in Figure 6a the HCl-induced titration is shifted upward to a pK_a value of 4.6 ± 0.2. The titration kinetics (Table 1) exhibit both fast components. However, only a single slow component, similar in decay rate to S_1 (see Table 1), was observed. The relative amount of the fast component $A(F)/[A(F) + A(S)]$ follows a bell-shaped curve (Figure 6b) analogous to those reported in Figure 4. The rates and relative amplitudes of the two fast components were found to be essentially identical to those observed for the nondeionized (low pK_a) systems. As shown in Table 1 a jump to pH 3.5 (deionized) yields values for $k(F_1)$ and $k(F_2)$, as well as for $A(F_1 + F_2)$, which are similar to those obtained for a pH jump to pH 3.3 for the nondeionized system. Similar jumps from $pH_i = 6.0$ were also carried out to the final pH_f values of 4.0, 4.5, and 5.0. The values observed for $k(F_1)$ (25.0 ± 5.0, 24.0 ± 5.0, and 33 ± 5.0, respectively) and $k(F_2)$ (3.5 ± 1.0, 3.1 ± 1.0, 2.4 ± 1.0, respectively), are pH_f independent and analogous to those observed for $pH_f = 3.5$. The same applies to the intrinsic ratio between the two fast processes which was found to be essentially the same ($A(F_1)/A(F_1 + F_2) = 0.8 \pm 0.05$) in all cases.

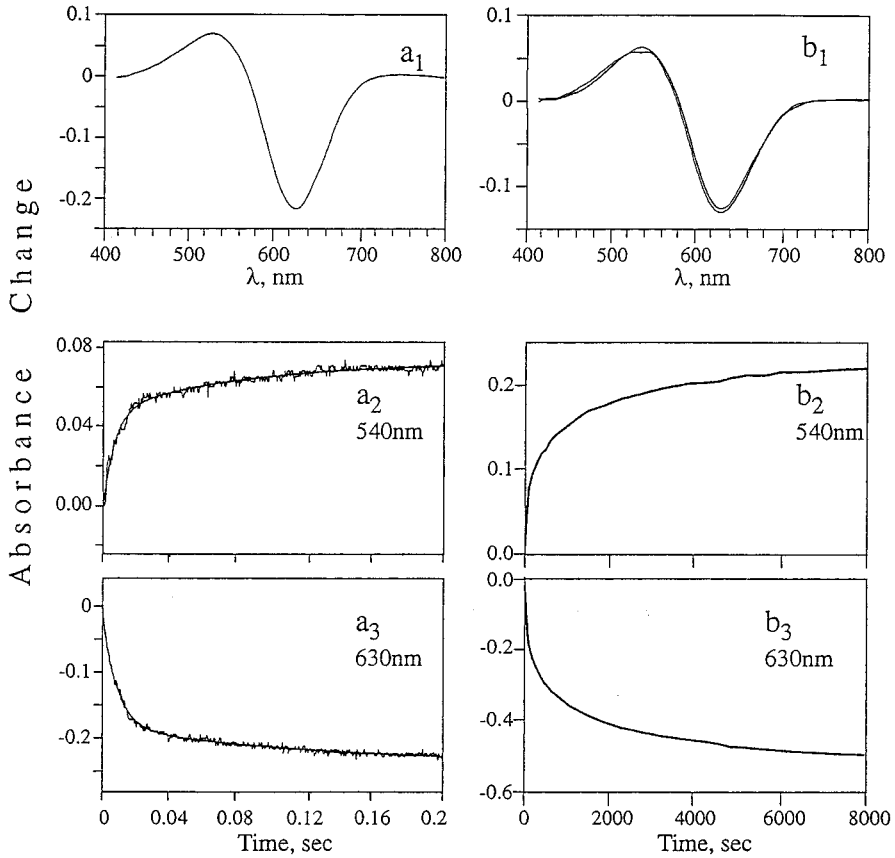

FIGURE 7: Characteristic different spectra (a_1,b_1) and kinetic traces (a_2, b_2, a_3, b_3) showing the pH-induced transition from blue bR (pH_i = 2.6) to purple bR (pH_f = 3.6). The initial suspensions at pH = 2.6 were prepared by adding $CaCl_2$ ([Ca^{2+}]:[bR] = 10:1) to the deionized systems as described in the text. (a_1 to a_3) Fast components (<3 s); (b_1 to b_3) slow components (>3 s).

Blue to Purple Transitions. The equilibration kinetics between the Blue and Purple forms of bR was also investigated by performing pH jumps in the opposite direction, namely, from low pH (pH_i = 2.6) to higher pH values (up to pH_f = 7.2). A problem when working with bR suspensions at low pH is the aggregation phenomena associated with substantial scattering. We have found that aggregation phenomena around pH = 2.6 are substantially inhibited when the blue, low-pH, bR suspension is prepared by first deionizing the system by passing it through the cation-exchange column and subsequently adding a controlled amount of Ca^{2+} (10:1 [$CaCl_2$]:[bR]). The resulting solution exhibits the same Purple⇔Blue pK_a value as that of the non-deionized bR system (as well as of solutions with higher [Ca^{2+}]:[bR] ratios; see below). An additional advantage of this titration procedure is that pH jumps from low pH (blue) bR to high pH (purple) bR (both in the presence of 10:1 [$CaCl_2$]:[bR]) can be directly compared with Blue→Purple transitions induced by cation jumps rather than by pH jumps. Such cation jumps, which will be described below, lead to final solutions with controlled pH_f and [Ca^{2+}]:[bR] ratios, which can be set to match the final conditions of the Blue to Purple pH jumps with a defined [Ca^{2+}]:[bR] ratio. This is obviously not possible when the pH jumps are performed in nondeionized bR solutions carrying a noncontrolled amount of Ca^{2+} ions.

Characteristic kinetic traces showing the Blue to Purple pH jumps, to pH_f = 3.6, are given in Figure 7. It is evident that the basic features reported above for the opposite (Purple to Blue) titration, namely, the multicomponent nature of the titration, are maintained in these low to high pH jumps. Characteristic kinetic parameters are presented in Table 1. For the jump to pH_f = 3.6 the four component analysis yields a $k(F_1)$ value (70 ± 10 s^{-1}) which is of the same order of magnitude as that of the opposite (Purple to Blue) titration to pH = 3.3 ($k(F_1)$ = 32.0 s^{-1}). The same applies to the F_2 component (0.4 s^{-1}, vs 1.0 s^{-1}). However, it appears that the relative amplitude of F_2 ($A(F_2)/A(F_1 + F_2)$ = 0.46) is higher than that (0.20) observed for the Purple to Blue transition.

In Figure 8a the total amplitude (A) and the relative amounts of the fast and slow decay components are plotted as function of the final pH. It is evident that the overall amplitude exhibits a titration curve with a pK_a value (pK_a = 3.3 ± 0.2) which is the same as that measured in the opposite, Purple to Blue titrations (Table 2). However, the relative amplitudes of the various components show an additional pH effect which occurs in the range between pH = 4.5 and pH ∼ 7. Upon increasing the pH the fast components increase at the expense of the slow components which become essentially negligible at pH ≈ 7. As to the rate parameters, no marked pH dependence on the various rate components was found in the range between pH 3.2 and 6.

(II) Cation Jumps

As discussed above it is well established that the Purple⇔Blue transition is affected both by pH and by the concentration of metal ions. We have thus carried out a series of time-resolved experiments in which the Blue to Purple transition is induced by cation jumps rather than by the previously described pH jumps. Figure 9 shows characteristic kinetic traces associated with a cation jump in which 50 equiv of $CaCl_2$ was added to a deionized (blue) bR membrane suspension. The initial pH of the blue

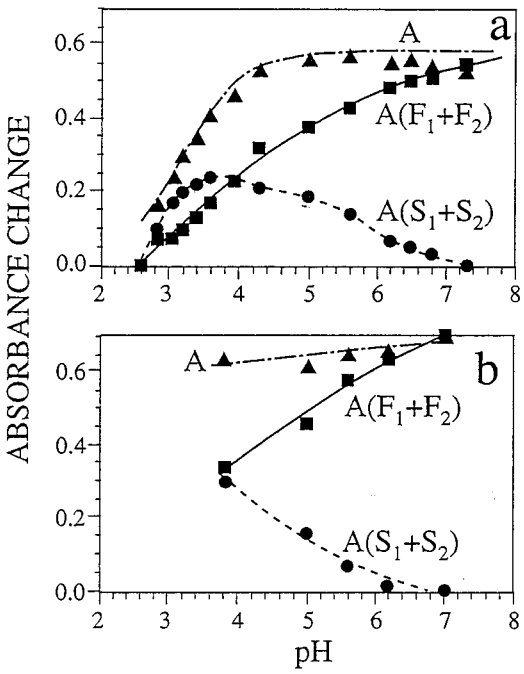

FIGURE 8: pH dependence of the relative amounts of the various components of the Blue→Purple transition. (a) pH jumps (initial conditions are as in Figure 6). (b) Cation (Ca^{2+}:bR, 10:1) jumps ($pH_i = 4.0-4.2$).

membrane suspensions, prepared by passing the (purple) bR membranes through the cation-exchange column, was in the range between 4.0 and 4.2. The final pH, after 1:1 mixing with the $CaCl_2$ solution, was 3.7−3.9. In keeping with the work of Zubov et al. (1986) multiphasic decay patterns are observed which are reminiscent of those described above for both Purple to Blue and Blue to Purple pH jumps. The decay constants and the respective amplitudes obtained by a four-component analysis in the case of a characteristic 10:1 [Ca^{2+}]:[bR] jump are given in Table 1. Analogous experiments were carried out for a series of final Ca^{2+} concentrations as well for several other metal ions (Na^+, Mg^{2+}, Eu^{3+}). The respective kinetic data, given in Table 3, show that the basic rate and amplitude parameters are essentially independent of the concentration and nature of the specific ion involved. The ∼100-fold concentrations employed in the case of Na^+ are implied by its much lower binding constant to the high-affinity binding sites of bR (Kimura et al., 1984; Jonas & Ebrey, 1991).

It has been reported that the isomer composition of dark-adapted Blue bR is 1:1 *all-trans:*13-*cis* (Smith & Mathies, 1985). Due to difficulties associated with the very fast light to dark adaptation of blue bR (Balashov et al., 1993) the isomer composition in the light-adapted state has not yet been established. Nevertheless, to probe the effect of the state of retinal isomerization on the Blue to Purple cation jumps, experiments were carried out exposing the blue membrane in the stopped-flow syringe to intense white light. The cation jumps were performed immediately (≤1 s) after turning off the light source. The maximum amplitudes of the $A(F_1 + F_2)$ difference spectrum of the light-adapted samples were found to be red shifted to 552 and 632 nm (compared to 532 and 626 nm, respectively, in the dark-adapted suspensions). This is indicative of an isomer composition which is richer in the *all-trans* component (though not essentially 100% *all-trans*, as it is the case for light-adapted purple membranes at higher pH values). The kinetic rate parameters of such jumps are given in Table 1 along with those of the

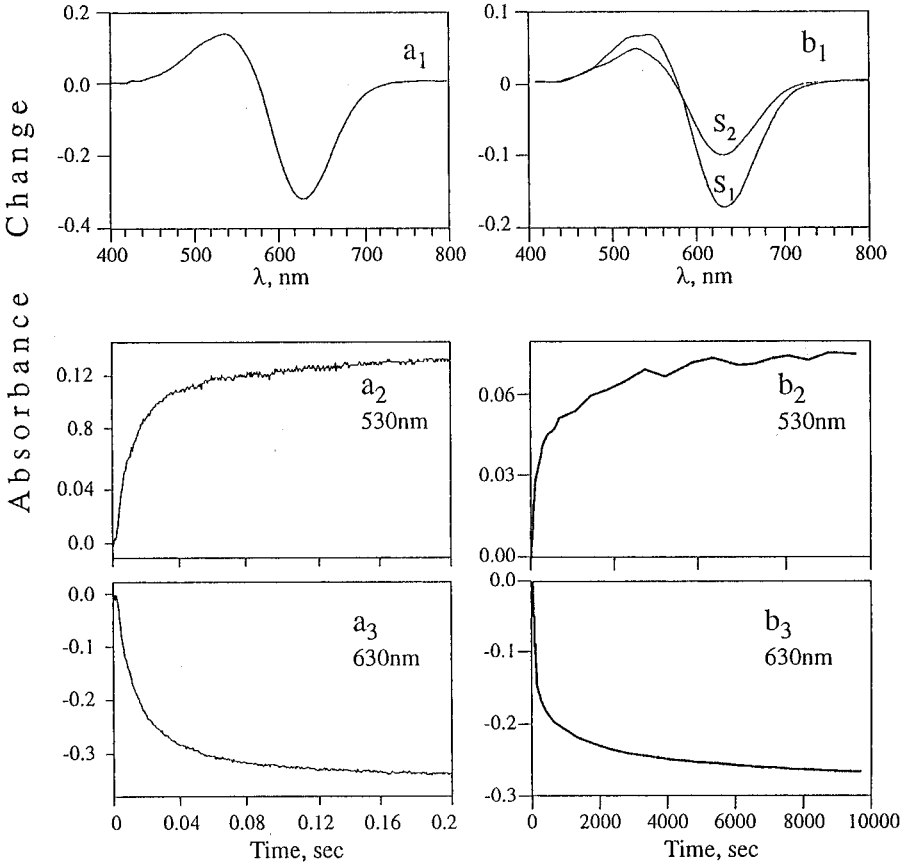

FIGURE 9: Kinetic traces and difference spectra showing the formation of purple bR following 1:1 mixing of deionized bR ($pH_i = 4.2$) and 50:1 [$CaCl_2$]:[bR], solutions ($pH_f = 3.8$). (a_1) F components; (b_1) S_1 and S_2 components; (a_2, a_3) stopped-flow traces; and (b_2, b_3) spectrophotometer traces.

Table 3: Kinetic Parameters Characterizing the Blue→Purple Transition Induced by Various Cation Jumps[a]

		Ca^{2+}				Mg^{2+}				Na^+		Eu^{3+}	
		1:1	2:1	10:1	50:1	1:1	2:1	10:1	50:1	500:1	5000:1	2:1	5:1
F_1	k	60	60	64	66	64	64	64	72	53	63	70	98
	A	0.27	0.31	0.25	0.49	0.33	0.30	0.40	0.48	0.37	0.51	0.38	0.61
F_2	k	0.5	0.18	0.8	0.59	0.71	0.51	0.34	0.69	2.16	0.65	1.26	0.85
	A	0.05	0.09	0.16	0.22	0.17	0.14	0.19	0.22	0.12	0.16	0.10	0.19
S_1	k	3.4×10^{-2}	2.2×10^{-2}	1.3×10^{-2}	3.0×10^{-2}	2.9×10^{-2}	2.1×10^{-2}	1.5×10^{-2}	2.4×10^{-2}	3.5×10^{-2}	3.5×10^{-2}	4.1×10^{-2}	4.3×10^{-2}
	A	0.26	0.24	0.29	0.21	0.27	0.23	0.12	0.22	0.14	0.20	0.27	0.14
S_2	k	1.0×10^{-3}	1.6×10^{-3}	5.61×10^{-4}	5.3×10^{-4}	8.1×10^{-4}	7.5×10^{-4}	9.1×10^{-4}	7.5×10^{-4}	1.4×10^{-3}	1.1×10^{-3}	1.1×10^{-3}	1.1×10^{-3}
	A	0.42	0.36	0.30	0.08	0.23	0.33	0.29	0.06	0.37	0.13	0.25	0.06

[a] $pH_i = 4.0-4.2$, $pH_f = 3.7-3.9$. Ratios represent the [cation]:[bR] molar ratio. k values are in s^{-1}.

dark-adapted suspensions. It is evident that the different isomer composition does not affect substantially the kinetics of the F and S_1 components. This conclusion is analogous to that derived above in the case of the F components of the opposite, Purple to Blue, transitions induced by pH jumps. Since the kinetics of light→dark adaptation occur on a time scale which is comparable to that of S_2, a similar conclusion is still precluded in the case of this component.

As reported above, substantial pH effects were observed in the case of Blue→Purple pH jumps, starting with non-deionized suspensions adding $CaCl_2$ + NaOH (Figure 8a). We have carried out analogous experiments starting from deionized blue membranes ($pH_i = 4.0-4.2$). The relevant amplitude data are given in Figure 8b. It is evident that an increase in $A(F_1 + F_2)$ and a corresponding decrease in $A(S_1 + S_2)$ occur upon increasing the pH from 4 to 7. The effect is analogous to that (Figure 8a) reported above in the case of the pH-induced Blue→Purple transition. Interestingly, an increase by a factor of ~4 is also observed for both $k(F_1)$ and $k(F_2)$ in the 5−7 range.

Experiments (with low time resolution) have been also carried out in which the reverse Purple→Blue transition was induced by a deionizing cation jump. For this purpose we first prepared a purple bR preparation in which all cations were replaced by potassium by adding 0.1 N KOH to a deionized (blue) bR membrane suspension to final concentrations of $[KOH] = 1.2 \times 10^{-3}$ M, $[bR] = 1.6 \times 10^{-5}$ M. This preparation was mixed with an equal volume (and equal pH) of a 0.4 M 18-crown-6 solution to final pH values of 4.0, 4.5, and 5.0. In all cases we observed a single slow component with a predominant fast component $A(F) = 0.8$ (Table 1). These patterns are similar to those characterizing the reverse Purple→Blue transition induced in deionized bR by pH jumps as reported above (see also Table 1, footnote *c*).

DISCUSSION

Multiphasic Nature of the Kinetics of the Blue⇔Purple Transition: Previous Approaches

Any analysis of the titration of Asp-85 in bR should first address the mechanism underlying the multicomponent kinetics of the Blue⇔Purple transition. The two fast components F_1 and F_2 were first observed by Druckmann et al. (1981) for pH pumps from purple bR (pH 7) to blue bR (pH 2.1−2.7). Our present results indicate a more complex equilibration kinetics, requiring the inclusion of the two additional slow components S_1 and S_2. Moreover, the same patterns are also shown to characterize the opposite, Blue to Purple, pH jumps. In the case of Blue to Purple transitions induced by cation jumps, three kinetically distinct steps have been previously reported by Zubov et al. (1986). As described above, such kinetics are now best described in terms of a four-exponent analysis. Two major observations should be taken into account when attempting to interpret such multicomponent kinetics. First, that analogous (though not exactly identical) kinetic patterns are observed for both Purple to Blue and Blue to Purple equilibration processes. Second, that such patterns are maintained independently on whether the transitions are induced by pH jumps or by ion jumps. Both analogies qualitatively apply to the rates and to the relative amplitudes of the four components and are clearly evident when pH or cation jumps, in either direction, are carried out to the same final pH (Table 1).

A previous approach, accounting for the multiphasic kinetics of Purple to Blue pH jumps, suggested cooperativity effects on the basis of the trimer structure of bR in the purple membrane (Druckmann et al., 1985). Accordingly, the fast titration of two of the trimer members (F_1) affects the structure of the third, resulting in a slow rate component (F_2) for the last third of the titration. This approach is inconsistent with the present observation of similar kinetic features for the opposite (Blue to Purple) titration, with the four (rather than two) components, and with the effects of pH on their relative amounts. Primarily, the trimer approach is inconsistent with the presence of the additional components, S_1 and S_2. In the case of Blue to Purple cation jumps, the multiphasic kinetics were explained by a reaction scheme involving a pre-equilibrium of blue-bR with a (blue) precursor of the final purple form (Zubov et al., 1986). This model predicts a dependence of the fast component (F_1) on the metal concentration, which is in variance with the data of Table 3. Moreover, it cannot account for the observation that analogous kinetics characterize the Blue⇔Purple equilibration, independently of the direction of the titration and of the nature of the inducing concentration jump (pH or cation). Another feasible possibility is that the multi-exponential titration kinetics is related to the *all-trans*:13-*cis* heterogeneity of bR. This possibility is readily excluded by the absence of substantial effects of light−dark adaptation on the pH-induced and cation-induced kinetics, as well as by most of the arguments presented above with relation to the trimer and pre-equilibrium mechanisms.

Proposed Titration Mechanism

As outlined in the introduction, two major approaches have been proposed to account for the pH and metal cation effects on the Purple⇔Blue equilibrium. One approach (model a) claims that free or bound metal cations on the membrane surface compete with protons and thus determine the local proton concentration at the binding site, which determines

the state of protonation of Asp-85 (Chang et al., 1986; Kimura et al., 1985; Ariki et al., 1987; Concoran et al., 1987; Dunach et al., 1987; Szundi & Stoeckenius, 1987, 1988, 1989). The second approach (model b) attributes the above effects to the competition between protons and metal cations on a specific binding site (not essentially on the surface) associated with two protein groups, Y and Z (Ariki & Lanyi, 1986; Jonas & Ebrey, 1991; Zhang et al., 1992; Stuart et al., 1995; Birge et al., 1996). More specific versions of model (b) identify Y as Asp-85 (Jonas & Ebrey, 1991; El-Sayed et al., 1995; Stuart et al., 1995; Birge et al., 1996) and Z as Asp-212 (Jonas & Ebrey, 1991). The latter assignment has, however, been put into question on the basis of NMR data indicating that in the blue form Asp-212 is still deprotonated (Metz et al., 1992). Some of the models also include a direct interaction of the metal ion with the Schiff base (Jonas & Ebrey, 1991; El-Sayed et al., 1995) while others (Birge et al., 1996) do not. These class b models imply that the apparent pK_a of Asp-85 is determined by the cation concentration. Accordingly, high and low pK_a values are observed in the absence and presence of cations, respectively. In other words, protons and metal ions compete on the Y, Z binding site determining the state of protonation of Asp-85. Obviously, a combination of the two models is also possible. We note that according to model b it is possible that the apparent pK_a of the titration is that of the Z^- (and Y^-) metal binding group(s) rather than that of Asp-85 itself.

It is important to emphasize that our present time-resolved titration data do not contribute to a clear discrimination between the above two models.[2] Thus, in the subsequent discussion we shall concentrate on the titration mechanism *after* the titration has been triggered, either according to model a or to model b. In both cases the trigger is binding/unbinding of a metal cation and the complementary unbinding/binding of one or more protons. The observation (Table 3) that the multicomponent kinetic features of the Blue→Purple, cation-induced reaction are totally independent of the nature and concentration of the metal cation indicates that the metal binding/unbinding process is not rate determining, neither in the trigger step nor in the subsequent Asp-85 deprotonation/protonation step. Accordingly, the simplest approach is to assume that the kinetics of the titration of Asp-85 are controlled by its protonation/deprotonation rates, implying that it is this very process which exhibits the multicomponent kinetics.

When attempting to rationalize such complex kinetic features we first note that in variance with elementary acid−base equilibria, the titration kinetics of protein residues may exhibit complex features [see Honig et al. (1995)]. In a previous analysis (Druckmann et al., 1995), we have shown that a titrable protein residue can behave as a "free" acid−base moiety, for which the observed protonation or deprotonation rate constant is given by the expressions

$$k(\text{obs}) = k_d + k_a[H^+] \quad (1)$$

$$K = k_d/k_a \quad (2)$$

where k_d and k_a are dissociation and association rate constants and K is the thermodynamic equilibrium constant. This was found to be the case for the titration of the Schiff base of an artificial bR in the pH 7−9 range. Alternatively, the titration rate of a protein residue may be controlled by the pH-independent rate of proton transfer through an appropriate channel. This mechanism was proposed in the case of the titrations of the Schiff base and of Asp-85 at relatively low (<7) pH_f values.

In variance with our previous analysis, in which the titration of Asp-85 was treated as a single-component reaction (Druckmann et al., 1995), we now have to account for considerably more complex kinetic patterns, specifically for the observation of four kinetic components and, primarily for the pH dependence of their relative amplitudes and rates. *We approach these phenomena by suggesting that the rate of protonation or deprotonation of Asp-85 is controlled by the rate of proton transfer through a specific channel. Accordingly, the multicomponent kinetics are attributed to the presence of several protein states, and thus of several proton channels, determined by the state of protonation of protein residues.* This approach is preferred over the alternative approach, namely, the "free" acid−base equilibrium (eq 1), because of two major arguments. First, as mentioned above, in the case of the SB titration eq 1 does not hold below pH 7. Since the SB and Asp-85 appear to be titrated through the same proton channel (Druckmann et al., 1985, 1995; Kataoka, et al., 1994), this will also apply to Asp-85. Second, eq 1 predicts that the observed titration rate should depend on k_d, i.e., on K. We have shown that the rate of the fast component of the Asp-85 titration, $k(F_1)$, is essentially unchanged in the cases of a synthetic aromatic bR pigment and of the bR mutant R82Q exhibiting Asp-85 pK_a values (5.2 and 7.0, respectively), which are substantially higher than that of the native pigment (Druckmann et al., 1985).

It is evident that the major challenge when attempting to rationalize the multicomponent titration features of Asp-85 in terms of a multiple channel approach, is to provide a molecular description of the related structural (channel) heterogeneity. The marked pH effect on the relative weights of the various components (Figures 4, 5, and 7) clearly suggests that such channel heterogeneity is pH-controlled and may thus be attributed to the titration of several protein residues. Consider for example the pH-induced Purple to Blue titration fractions shown in Figure 4. The two fast components predominate at high pH. As the pH is lowered they decrease, passing through a minimum and rising again at still lower pH values. The two S components exhibit an opposite, complementary, behavior but are shifted relative to each other. The simplest model to account for this behavior is to assume that there are two protein groups, A_1 and A_2, that control the proton channel to Asp-85 by giving rise to four pH-dependent protein states:

State I:	A_1^-, A_2^-	F channels
State II:	A_1H, A_2^-	S_1 channel
State III:	A_1^-, A_2H	S_2 channel
State IV:	A_1H, A_2H	F channels

It is impossible to account for the rise and fall of A_{S1} and A_{S2}, or for the lag of A_{S2} after A_{S1}, with only two titrations. Thus, to avoid the complications associated with an ad-

[2] According to the present observations the trigger step, associated with the binding/unbinding of metal ions, does not affect the titration rates even in the case of a large trivalent cation such as Eu^{3+}. This would be difficult to reconcile with model b binding sites which are not close to the membrane surface.

Scheme 1

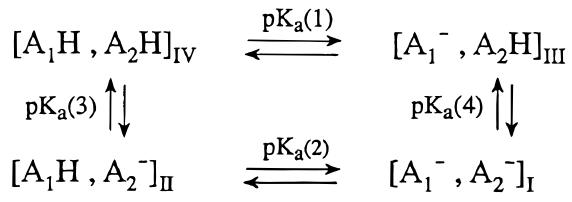

ditional group (A_3), we have assumed a simple model in which the two groups A_1 and A_2 are interactive according to Scheme 1, where one allows for different values for the various pK_a's which will be complex functions of the mutual states of protonation as well of the specific anion involved. Figure 4 compares the relative weights of the four states (I−IV) calculated according to Scheme 1, with our experimental points for A_F, A_{S1}, and A_{S2}, in the case of the various anions used in the acidification experiments. The fitted pK_a values are given in Table 2, along with those of the overall titrations. It is evident that Scheme 1 yields very good agreement with our experimental data for all of the anions employed. We note that the model of Scheme 1, in which the pK_a of a protein residue depends on the state of protonation of another residue, was first applied to bR by Balashov et al. (1995, 1996) to account for the pH-dependence of the Purple⇔Blue transition and for the Asp-85-catalyzed *trans*→13-*cis* isomerization. In that case, the intergroup interaction between the two groups (Asp-85 and Glu-204) leads to larger differences between the various pK_a values then those shown in Table 2. Evidently the interactions between A_1 and A_2 appear to be smaller than those between Asp-85 and Glu-204.

There are several points which should be emphasized with relation to the model of Scheme 1:

(a) The model implies that, for the same pH_f and $[M^{2+}]$ conditions, similar kinetics (controlled by the protonation/deprotonation of Asp-85) will be exhibited by both Purple→Blue and Blue→Purple equilibration reactions. Moreover, this should apply independently on whether the reactions are induced by proton- or by metal−concentration jumps. As shown, e.g., in Table 1 this prediction is basically in keeping with our observations.

(b) According to the proposed model the channel-controlling titrable groups, A_1 and A_2 differ, from the metal binding groups, Z and Y, which determine the effective pK_a of Asp-85. However, modified versions of the model can also account for the cases that Z and/or Y may be identified with A_1 and/or A_2. At the present stage of the investigation this possibility cannot be excluded.

(c) Another inherent assumption is that the acid−base equilibration of the A_1 and A_2 groups is faster than that of $Asp85^-$, i.e., it is completed on a time scale of less than several milliseconds.

(d) An interesting feature of the postulated pK_a values, both of the overall titration (i.e., of Z^- and Y^-) and of the rate-controlling groups, A_1 and A_2, is their dependency on the specific acid involved. This suggests that the corresponding anions are bound in the vicinity of the titrable groups, affecting their pK_a values.

(e) An important factor which affects both the overall titration pK_a, as well as those of A_1 and A_2, is the salt concentration. Thus, in our deionized bR preparations the apparent pK_a of the titration is raised from below 3.5 to about 4.5 (Figure 6). Similarly, the "bell-shaped" curves in Figure 6 exhibit a comparable upward shift with respect to the nondeionized system (Figure 4). It appears that the pK_a values of A_1 and A_2 in the deionized system change in a way that shifts the "bell-shaped" curve, as well as decreases the maximum value of A_S and increases the minimum value of A_F. An analysis of these data in terms of the model of Scheme 1 yields very good agreement, yielding the pK_a values given in Table 2. The presence of only one S component may be rationalized by assuming that in the deionized system S_1 and S_2 exhibit similar k values. Alternatively, it is also possible that the complete absence of the S_2 component in the deionized system is due to a very large upward shift of the pK_a of A_2. In any event, these observations suggest that metal ions induce an upward shift not only in the pK_a of the overall titration (e.g., of Y^- and Z^-), but also in those of the rate-controlling groups, A_1 and A_2. It is tempting to suggest that A_1 and A_2 are associated with the second strong metal binding site in bR (El-Sayed et al., 1995).

It is worthwhile recalling that while the total relative contribution of the two fast components (A_F) and those of the two slow components (A_{S1} and A_{S2}) are pH dependent, no substantial effects were found on the intrinsic fractions of the two fast components $A(F_1)/A(F_1 + F_2)$ and $A(F_2)/A(F_1 + F_2)$. (The relative contribution of F_2 varies in the range $A(F_2)/A(F_1 + F_2) = 0.2-0.5$, depending on the specific system; see Tables 1 and 3.) This implies that a model based on a pH-induced heterogeneity cannot be applied in order to account for the biphasic nature of the fast processes. At present we are still incapable of presenting a feasible explanation for the biphasicity of the fast reactions.

Having discussed the pH dependency of the amplitudes of the various titration components, one should consider the effects of pH on the rate constants pertaining to such components. As shown in Figure 5 there appear to be two classes of pH effects on these rates. The first (Figure 5b,c) concerns $k(S_1)$ and $k(S_2)$. In variance with the pH independency of $k(F_1)$ and $k(F_2)$ (Figure 5a), both slow rate components exhibit a sharp rise below pH 3. One possibility is that an additional low pK_a group is protonated affecting the H^+ channel efficiency of S_1 and S_2. This explanation, which means adding two additional low pH channels, S'_1 and S'_2, implies a pH-dependent biphasicity in each of the two slow components which may be difficult to detect. Alternatively, we cannot exclude the possibility that in S_1 and S_2 (but not in F_1 and F_2) the titration follows eq 1 with k_d predominating at high pH and k_a $[H^+]$ at low pH. The pH effect on the fast components observed between pH ∼ 6 and pH ∼ 7 is opposite to that on $k(S_1)$ and $k(S_2)$, namely, $k(F_1)$ and $k(F_2)$ increase upon lowering the H^+ concentration. Here again the effect may be rationalized by invoking an additional titration of a protein residue with pK_a ≈ 6. This phenomenon will be addressed in future work.

CONCLUSIONS

On the basis of the complex time-resolved titration features of Asp-85 in bR, we suggest that the protonation/deprotonation kinetics of this key residue are determined by the existence of several states of the protein which give rise to several corresponding proton channels. These are determined by the state of protonation of at least two protein groups A_1 and A_2. The latter, kinetics-controlling, groups may, or may not, differ from the groups (Y and Z) which determine the effective pK_a of Asp-85. The pK_a's of all four residues are

affected by deionization and may thus be associated with the stronger-binding cation sites.

Although in accord with our experimental observations, the proposed model must be quantitized to account for several features which are presently unclear, including the observation that the relative weight of the slow components, at pH $\sim$ 4, in the Blue→Purple transition (Figure 8) is considerably higher than in the case of the opposite, Purple→Blue jumps to the same pH (Figure 3). This may imply the existence of a protein residue whose state of protonation, which depends on the initial conditions of the titration, affects the pK_a values of A_1 and A_2. However, the major outstanding problem is the specific assignment of the various residues involved with the titration of Asp-85, including the identification of Y and Z with Asp-85 and Asp-212 (Jonas & Ebrey, 1991). Relevant information in this respect may be derived from future experiments in which the kinetics of the H^+ and M^{2+} exchange processes will be resolved and compared to those of the Purple⇔Blue transitions. The nature of A_1 and A_2 may be approached by studying the Blue⇔Purple equilibration kinetics in bR mutants. Plausible candidates are groups such as Glu-74, Glu-9, and Glu-194 located on the extracellular side of the chromophore binding site (Grigorieff et al., 1997).

Although related to bR in its resting (unphotolyzed) form, the present observations bear on the function of bR as a light-induced proton pump. The latter is based on proton channels, to and from SBH^+ and Asp-85, which are controlled by structural changes in the protein during the photocycle [see e.g., Honig et al. (1995)]. The concept that such channels may be controlled by the titration of selective protein residues (such as A_1 and A_2), which are in turn affected by metal ions, may provide new insights into the molecular mechanism of the light-induced proton pump.

REFERENCES

Ariki, M., & Lanyi, J. K. (1986) *J. Biol. Chem. 261*, 8167−8174.

Ariki, M., Magde, D., & Lanyi, J. K. (1987) *J. Biol. Chem. 262*, 4947−4951.

Balashov, S. P., Govindgee, R., Kono, K., Imasheva, E., Lukashev, E., Ebrey, T. G., Crouch, R. K., Menick, R., & Feng, Y. (1993) *Biochemistry 32*, 10331−10343.

Balashov, S. P., Govindgee, R., Imasheva, S., Misra, S., Ebrey, T.G., Feng,Y., Crouch, R. K., & Menick, D. R. (1995) *Biochemistry 34*, 8820−8834.

Balashov, S. P., Imasheva, E. S., Govindgee, R., & Ebrey, T. G. (1996) *Biophys. J. 70*, 473−481.

Birge, R., Govender, D., Izgi, K., & Tan, E. (1996) *J. Phys. Chem. 100*, 9990−10004.

Brown, L. S., Sasaki, J., Kandori, H., Maeda, A., Needleman, R., & Lanyi, J. K. (1995) *J. Biol. Chem. 270*, 27122−27126.

Chang, C.-H., Chen, J.-G., Govindjee, R., & Ebrey, T. (1985) *Proc. Natl. Acad. Sci. U.S.A. 82*, 396−400.

Chang, C.-H., Jonas, R., Melchiore, R., Govindjee, R., & Ebrey, T. G. (1986) *Biophys. J. 49*, 731−739.

Concoran, T. C., Ismail, K. Z., & El-Sayed, M. A. (1987) *Proc. Natl. Acad. Sci. U.S.A. 84*, 4094−4098.

Druckmann, S., Samuni, A., & Ottolenghi, M., (1979) *Biophys. J. 26*, 143−145.

Druckmann, S., Ottolenghi, M., Pande, A., Pande, J., & Callender, R. H. (1982) *Biochemistry 21*, 4953−4959.

Druckmann, S. Ottolenghi, M., & Korenstein, R. (1985) *Biophys. J. 47*, 115−118.

Druckmann, S., Ottolenghi, M., Rousso, I., Friedman, N., & Sheves, M. (1995) *Biochemistry 34*, 12066−12074.

Dunach, M., Seigneuret, M., Rigund, J. L., & Padros, E. (1987) *Biochemistry 26*, 1179−1186.

El-Sayed, M. E., Yang, D., Yoo, S.-K., & Zhang, N. (1995) *Isr. J. Chem. 35*, 465−474.

Fischer, U., & Oesterheld, D. (1979) *Biophys. J. 28*, 211−230.

Grigorieff, N., Ceska, T. A., Downing, K. H., Baldwin, J. M., & Henderson, R. (1996) *J. Mol. Biol. 259*, 393−341.

Henderson, R., Baldwin, J. M., Ceska, T. A., Zemlin, F., Beckmann, E., & Downing, K. H. (1990) *J. Mol. Biol. 213*, 899−929.

Honig, B., Ottolenghi, M., & Sheves, M. (1995) *Isr. J. Chem. 35*, 429−446.

Jonas, R., & Ebrey, T. G. (1991) *Proc. Natl. Acad. Sci. U.S.A. 88*, 149−153.

Kataoka, M., Kamikubo, H., Tokunaga, F., Brown, L., Yamazaki, Y. Maeda, A., Sheves, M., Needleman, R., & Lanyi, J. K. (1994) *J. Mol. Biol. 243*, 621−638.

Kimura, Y., Ikegami, A., & Stoeckenius, W. (1984) *Photochem. Photobiol 40*, 641−646.

Masuda, S., Masayuki, N., Tasumi, M., El-Sayed, M. A., & Lanyi, J. K. (1995) *J. Phys. Chem. 99*, 7776−7781.

Metz, G., Siebert, F., & Engelhard, M. (1992) *FEBS Lett. 303*, 237−241.

Moore, T. A., Edgerton, M. E., Parr, G., Greenwood, C., & Perham, R. N. (1978) *Biochem. J. 171*, 469−476.

Mowery, P. C., Lozier, R. H., Chae, Q., Tseng, Y.-W., Taylor, M., & Stoeckenius, W. (1979) *Biochemistry 18*, 4100−4107.

Nakanishi, K., Balogh-Nair, V., Arnaboldi, M., Tsujimoto, K., & Honig, B. (1980) *J. Am. Chem. Soc. 102*, 7945−7947.

Oesterhelt, D., & Stoeckenius, W. (1971) *Nature (London) New Biol. 233*, 149−151.

Ottolenghi, M., & Sheves, M., Eds. (1995) Photophysics and Photochemistry of Retinal Proteins. *Isr. J. Chem. 35* (3−4), 193−515.

Scherrer, P., & Stoeckenius, W. (1985) *Biochemistry 24*, 7733−7740.

Smith, S. O., & Mathies, R. A. (1985) *Biophys. J. 47*, 251−254.

Subramaniam, S., Marti, T., & Khorana, H. G. (1990) *Proc. Acad. Sci. U.S.A. 87*, 1013−1017.

Stuart, J. A., Vought, B. W., Zhang, C.-F., & Birge, R. R. (1995) *Biospectroscopy 1*, 9−28

Szundi, I., & Stoeckenius, W. (1987) *Proc. Natl. Acad. Sci.* U.S.A. *84*, 3681−3684; (1988) *Biophys. J. 54*, 227−232; (1989) *Biophys. J. 56*, 369−383.

Warshel, A., & Ottolenghi, M. (1979) *Photochem. Photobiol. 30*, 291−293.

Zhang, Y. N., Sweetman, L. L., Awad, E. S., & El Sayed, M. A. (1992) *Biophys. J. 61*, 1201−1208.

Zimanyi, L., Váró, G. Chang, M., Ni, B. Needleman, R., & Lanyi, J. (1992) *Biochemistry 31*, 8535 −8543.

Zubov, B., Tsuji, K., & Hess, B. (1986) *FEBS Lett. 200* (1), 226−230.

BI970646C